15th Int Symp on Applications of Laser Techniques to Fluid Mechanics
Lisbon, Portugal, 05-08 July, 2010

Experimental investigation of the large scale flow structures around a trawl

Elkhadim Bouhoubeiny[1,3], Grégory Germain[1, 2], Philippe Druault[3]

1 ; IFREMER, Hydrodynamic & Metocean Service, 150 Quai Gambetta,
62321 Boulogne-sur-Mer, France, khadime@lmm.jussieu.fr; Gregory.Germain@ifremer.fr;
2 ; University Lille Nord de France, F-59000 Lille, France
3 ; University Pierre et Marie Curie-Paris 6, IJLRA, Case 162, 4 Place Jussieu,
75252 Paris cedex 5, France, philippe.druault@upmc.fr

Abstract.
Flow field measurements behind a rigid cod-end and a moving bottom trawl are conducted using Time Resolved PIV method. This method is based on an image acquisition rate allowing the time resolved sampling of the vortex shedding phenomenon. Based on such measurements, the main flow characteristics around fishing net structure are investigated. Moreover, the vortex shedding frequency phenomenon associated with both the rigid cod-end and the moving bottom trawl is analyzed. We then present the analysis of the instability of the shear layer separating a moving trawl having 3 degrees of freedom. Using also the Proper Orthogonal Decomposition (POD) for such investigation, it is demonstrated the effectiveness of this procedure to extract not only the large scale spatial flow structure but also their associated frequencies. POD is then shown to be robust to act as a filter for the frequency analysis.

1. Introduction

The analysis of hydrodynamics of various types of fishing net structures, and especially of a trawl, has been of great interest for scientists for a long time. Such investigation has an impact not only on commercial fishing operations including the fishing vessel energy efficiency but also on biological and socio-economical environment.
Due to the flexibility of the net, there is a complex interaction between flow, geometry (solidity) and shape of the net. In fact, the analysis of the hydrodynamic flow around (and also in) fishing net structures is extremely related to the strong influence of hydrodynamic fields on the shape of trawl elements, acting forces, fish behaviour and on catchability of fishing gears. The hydrodynamic turbulent flow has a great influence i) on the stability of the movement of the fishing net structure; ii) on the drag force of the fishing gear and iii) on selectivity (selectivity is the ability of fishing gears to prevent non-target fish catches). Due to his impact on fuel comsumption, the second point is more and more crucial for fishermen and researchers (Dahm *et al.* 2002; Priour 2009). The knowledge of these drag forces allows then the definition of the shape and the behaviour of the structure during a trawling process, and tension and loads in its threads and ropes (O'Neill *et al.* 2005). Globally, it is now well known that most of the fuel consumed during a fishing trip is used to tow the fishing gear and also that the trawls are responsible of the largest part of the fuel consumption during fishing operations. An important work should be done on this area to improve the energy efficiency of fishing gears. For instance, in designing a trawl net, fishing gear researchers often need to know the total drag force of the net to see if it fits the dynamics characteristics of the fishing vessel. In this sense, the HydroPêche project (Germain *et al.* 2010) has been launched in

order to develop a tool for automatic optimisation of trawl minimizing the drag of the gear. For that purpose, different aspects are studied in order: a/ to extend the basis of experimental data on flow characteristics governing the hydrodynamic behaviour of different porous structures, b/ to develop numerical tools to simulate more realistic flow around porous structures taking into account fluid/structure interactions and c/ to develop automatic optimisation tools to design efficient trawls in terms of energy consumption. This paper deals with the first aspect of this project, i.e. the experimental investigation of the turbulent flow around bottom trawls.

Despite its practical engineering application, there is almost no reported study on the analysis of hydrodynamic flow around a fishing net structure. Yet, it is clear that hydrodynamic flow has a very significant influence on the fish moving process. To investigate the flow in presence of a net and a catch (Fig. 1), Pichot *et al.* (2009) and Meyler (2008) previously used Laser Doppler Velocimetry (LDV) measurements to study the mean flow field over a rigid cod-end with a closed and an open net entrance. Other previous works have focused on the analysis of different mesh sizes or numbers to improve the selectivity without taking into account the hydrodynamic flow. Other previous experimental works have only focused on the measurement of the total drag force using empirical formulations based on numerous assumptions (O'Neill et al. 1997). Besides, the complexity of the flow makes numerical simulations difficult and today no effective model exists for such investigation. Indeed, such numerical computation needs to consider the following four issues: modelling the flow field, modelling the structural vibration, modelling the fluid-structure interaction and also the modelling of the net deformation. Furthermore, numerical simulations suffer from limitations due to a lack of experimental database that can be used to validate numerical results as well as numerical model, even if the results obtained for *classical* Vortex Induced Vibrations (VIV) analysis can be exploited. Indeed, due to the fundamental importance and the wide range of engineering applications, the hydrodynamic flow instabilities related to the VIV of a cylindrical or spherical structure have been extensively analyzed in the past (see for instance the reviews by Williamson and Govardhan 2004; Govardhan and Williamson 2005).

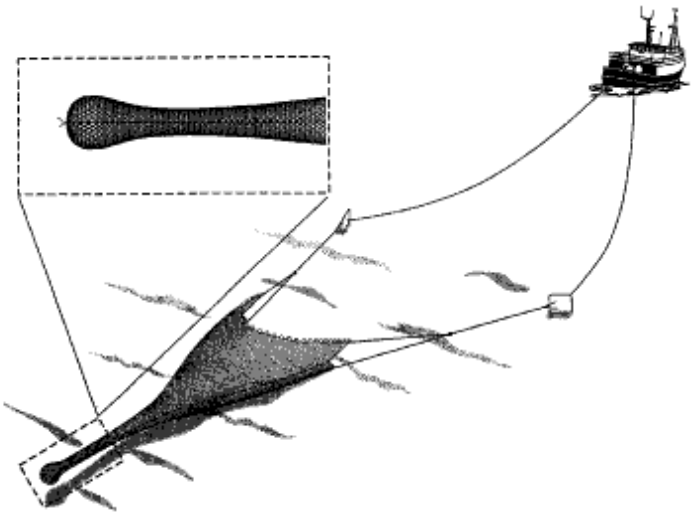

Fig. 1: Bottom trawl showing the position of the cod-end

To the author knowledge, we present one of the first studies aiming at investigating the instantaneous hydrodynamic flow around a porous structure. Two kinds of net structure are considered: a) a rigid cod-end and b) a 1/10 scale bottom trawl. Particle Image Velocimetry (PIV) is implemented to access the instantaneous velocity fields in each flow configuration.

To investigate the large scale flow structures around the trawl, specific mathematical post-processing procedure such as Proper Orthogonal Decomposition is applied. Part 2 of the paper is devoted to the experimental set up and measurement method. Part 3 deals with the mathematical post-processing tool use to analyze PIV database. Then after presenting global flow results, the large scale flow structure characteristics are examined in each flow configuration. Vortex shedding frequency analyses are performed and the influence of the movement of the trawl on flow dynamics is examined.

2. Experimental apparatus

2.1 Flume tank and fishing gear

Experimental campaigns are performed in the IFREMER (French Research Institute for Exploitation of the Sea) wave-current circulation flume tank shown in Fig. 1. Dimensions of the flume tank are 18 m (length) x 4 m (width) x 2 m (depth). A side observation window of 8 m by 2 m placed on one side of the tank allows users to observe the behaviour of the models during trials and to carry out video sequences. The bottom of the flume is a conveyor belt which can be synchronized with the water speed in order to simulate devices in contact with the bottom, like bottom trawls. The flow turbulence can be adjusted between 5 to 28 % and the flow streamwise velocity range is 0.1 to 2.2 m/s. In the following, measurements are performed with a fixed input streamwise velocity of U_{ref} = 0.54 m/s and a turbulence intensity rate of 5%.

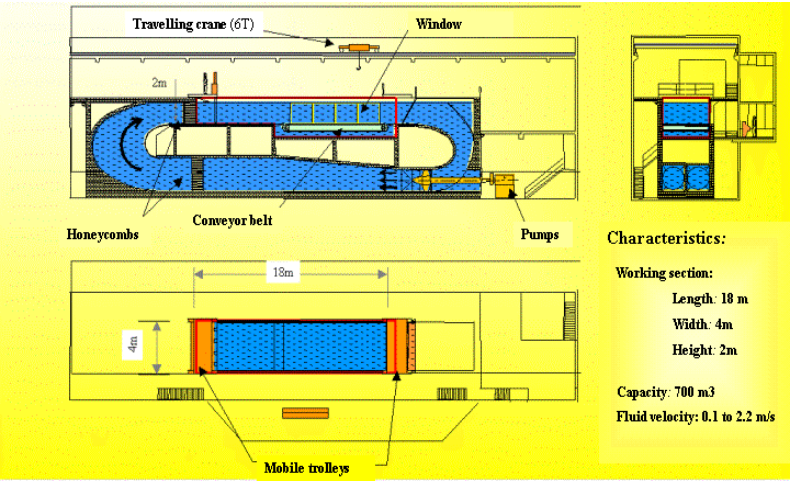

Fig. 2: Ifremer free surface hydrodynamic water tunnel

2.2 PIV system

In this study, Time-Resolved PIV (TRPIV) measurement method is used. The method that records the measurement of the existing velocities around fishing gear in the flume tank offers two main advantages: (1) it is non-intrusive and (2) it offers the possibility of mapping the velocities on one or more planes, in real time, and under unsteady conditions. This technique is based on illuminating the seeding particles and storing the resulting camera images to analyze displacements of particles between two successive images. The velocities are obtained by dividing the distance by the elapsed time of laser pulses. TRPIV is unique in providing data that can be used to extract not only spatial instantaneous flow structures but also frequencies associated with these flow structures. TRPIV database used for frequency analysis should satisfy the Nyquist criterion: database must then be sampled with at least twice the highest frequency present in the measurement signal. In this sense, we retain an

image acquisition rate allowing the time resolved sampling of the vortex shedding phenomenon.
The PIV system consists of a double pulsed laser type two-chamber Gemini PIV Nid-Yag 2 X120mJ at 15Hz, and a CCD camera Hi sense. In the flume tank, two cameras are available with two different objectives (focal lens). The first camera has a 4 Hz frequency, with a 1280 x 1024 pixels^2 resolution. The second one has a 15 Hz frequency, with a 1600 x 1200 pixels^2 resolution. Such frequency resolution allows then the investigation of the frequencies associated with the large scale flow structures.
The measurement plane corresponding to the focal lens length of 60 mm is 810.7 x 648.5 mm^2, while the measurement plane corresponding to the focal lens length of 20 mm is 387.91 x 290.843 mm^2. The image processing is done with the Flow Map 1500 software from Dantec dynamics. Finally, instantaneous velocity fields are obtained using a cross-correlation PIV algorithm. The interrogation windows size is 32x32 pixels^2 and adjacent windows are 25 % overlapped.

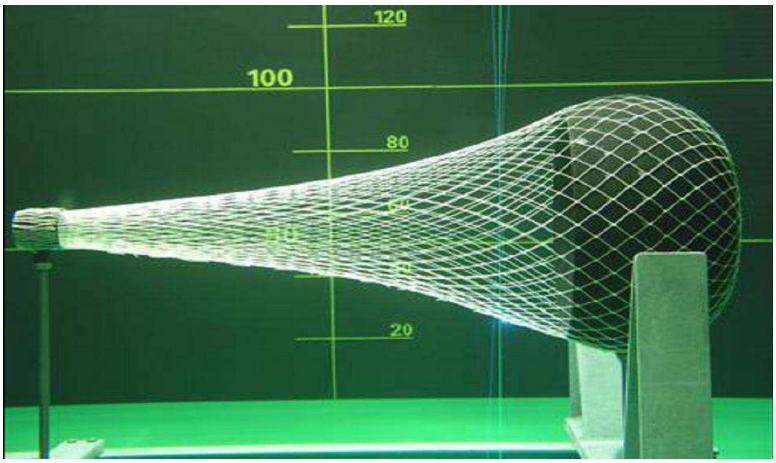

Fig. 3: Rigid cod end in the flume tank

2.3 PIV measurements

In this paper, we are going to investigate two different flow configurations. In each one, PIV system is implemented to determine the longitudinal *u* and transverse *v* velocity components along the y and z directions respectively.

The first flow configuration deals with the fishing gear using a rigid cod-end to avoid instabilities and to be able to characterize with accuracy the flow in this area (see Fig. 2). Previous measurements have been already obtained in such a flow configuration (Pichot *et al.*, 2009, Bouhoubeiny *et al.*, 2010). This structure is axi-symmetric and the catch inside the cod-end is limited by two spherical caps, so its shape is known. The model is 1m long, made of PA twine of 1200 m/kg, with diamond-shaped meshes of 30 mm lens.

The second flow configuration corresponds to the turbulent flow around a moving bottom trawl. The bottom trawl used for this study is a 1:10 scaled model of a 32.5 m swept width by 23.1 m swept height commercial bottom trawl. The diamond-shaped mesh size (twice the length of mesh side ISO 1107-1974) of the net is 8 mm, with a twine diameter of 0.6 mm.

2.3.1 Model rigid cod-end

In this flow configuration, the camera has a 15 Hz frequency with a 20 mm camera focal lens length. The size of the field is 387.91 x 290.843 mm^2 that is 1600 x 1200 pixels^2. The laser is placed above the catch of the net model and the camera is outside. Instantaneous velocity fields are obtained in several planes detailed in Fig. 3. The time between two images

is always 0.25s (4Hz) and 500 instantaneous images for each measurement plane are obtained. The spatial resolution is 5.5mm in both directions.

2.3.2 Model moving bottom trawl

In this configuration, the bottom trawl is free to move in the water flow. For such a test-case, the coveyor belt is synchronised with the flow speed. The laser is placed above the bottom trawl and the camera is outside. Instantaneous velocity fields are measured in selected planes along the bottom trawl. For each plane, 272 PIV images are stored. The time between two images is 0.067s (15 Hz). In this paper, only one measurement plane located behind the bottom trawl is investigated (see Fig. 4). On this Fig., two trawl positions corresponding to the bottom and the top ones respectively are also provided. An illustration of the TRPIV measurement is given on Fig. 5 where two instantaneous velocity vector fields are plotted. These vectors fields correspond to a different instant that is a different trawl position. Such representation clearly demonstrates the free movement of the trawl, not only in the transverse z-direction but also in the longitudinal y-direction (and also in the third direction that can not be visualized from 2D measurements).

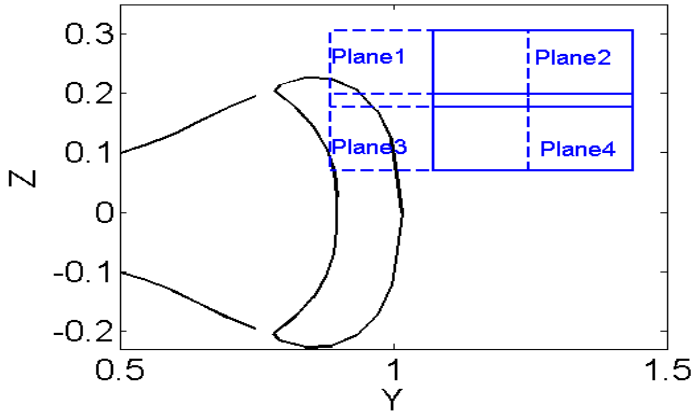

Fig. 3: Rigid cod-end measurements. Measurement planes. Overlapping planes 1-3 and 2-4 are represented in dotted lines and lines respectively.

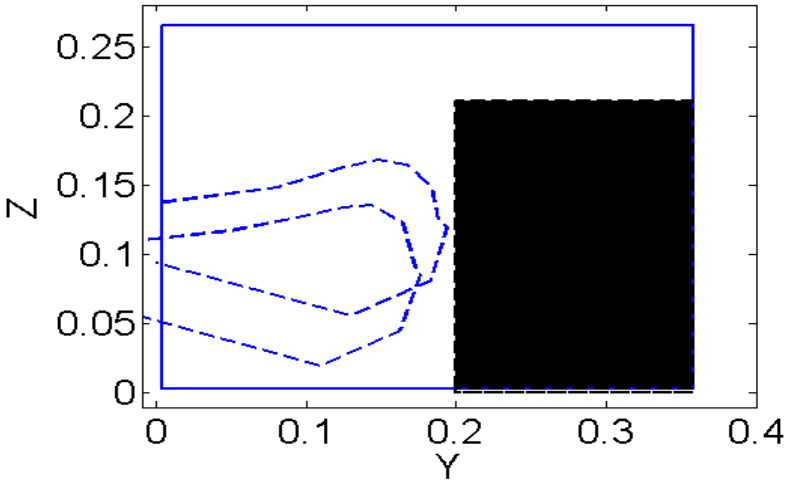

Fig. 4: Moving bottom trawl measurements. Measurement plane (blue line). Dot lines indicate the upper and lower z-positions of the bottom trawl during PIV measurements. Black box indicates the zone which is further investigated (section 4).

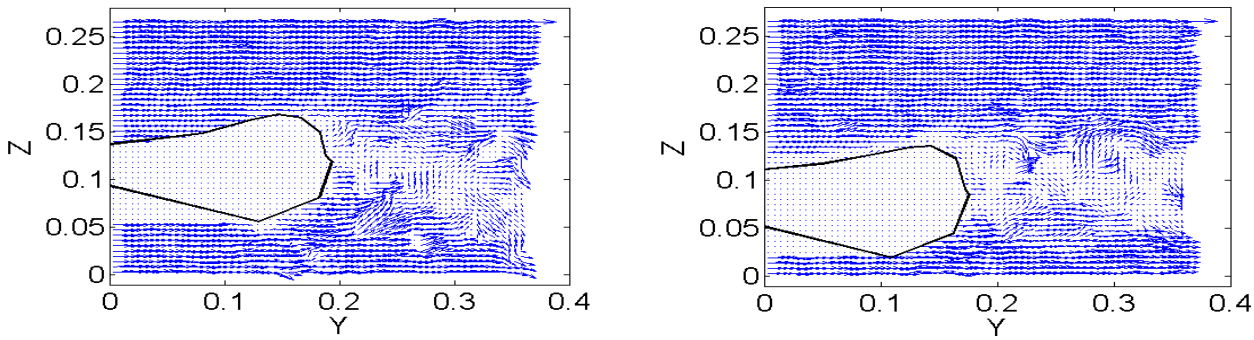

Fig. 5: Moving bottom trawl measurements : instantaneous vector fields obtained at two different instants.

3. Proper Orthogonal Decomposition (POD) mathematical tool

During the last two decades, POD procedure has become more and more a universal mathematical tool for turbulent flow analysis. Indeed, numerous POD applications have been shown its effectiveness in extracting energetic coherent structures of turbulent. The use of POD on PIV data has been reported in several publications recently. For instance, Huera-Huarte and Vernet (2009) used POD to reduce the dimensionality of the data for better investigating the wake of an oscillating flexible cylinder. Van Oudheusden *et al.* (2005) and Perrin *et al* (2007) used POD to obtain phase characterization of vortex shedding in the wake of a square section cylinder and of a circular cylinder respectively.

The application of Proper Orthogonal Decomposition to turbulent flow analysis was first proposed by Lumley (1967) as an objective method to identify deterministic features in turbulent flows. According to Lumley (1967), an organized flow structure called coherent structure is the structure that has the largest mean square projection of the velocity field. This maximization leads to a Fredholm integral eigenvalue problem (Holmes *et al.*, 1996)

$$\int R(X,X')\phi(X') = \lambda\phi(X), \tag{1}$$

where X indicates the vector space variable and $R(X,X')$ refers to the time averaged two point spatial correlation tensor of the velocity field. In this equation, ϕ denotes the spatial orthogonal eigenfunctions and λ is the corresponding eigenvalue. Such equation provides a finite discrete number of POD eigenfunctions, $\phi^{(n)}$ with n varying from 1 to N_{mod} which is the total number of POD modes corresponding to the dimension of the spatial correlation matrix. Based on this flow decomposition each instantaneous fluctuating velocity field (for instance the u velocity component) can then be expressed as follows:

$$u(X,t) = \sum_{n=1}^{N_{mod}} a^n(t)\phi^n(X), \tag{2}$$

where $a^{(n)}(t)$ is the n^{th} random temporal coefficient of projection of u(X,t) onto the n^{th} POD eigenfunction $\phi^{(n)}(X)$. Such previous development describes the classical formulation of the POD procedure. In this description, the dimension of the spatial correlation deduced from two-dimensional PIV images is the number of PIV grid points available on each flow image. Due to the possible high dimension of this kernel, an equivalent POD application has been performed by Sirovich (1987). This method called snapshot POD proposes to reduce the size of the POD eigenfunction problem in computing the eigenfunctions of the spatial average temporal correlation tensor. Finally such snapshot flow decomposition provides a similar expression of each velocity component (equation 2). Note that both classic and snapshot flow

decomposition provides orthonormal POD temporal coefficients: $a^{(n)}a^{(p)}=\delta_{np}$ with δ the Kronecker symbol and uncorrelated POD eigenfunctions satisfying $\phi^{(n)}\phi^{(p)}=\lambda^{(n)}\delta_{np}$.

POD is performed from each PIV database described above. The purpose of such application is to examine the turbulent flow field around the rigid cod-end and the moving bottom trawl, especially the POD effectiveness in extracting the large scale organized motion of the flow. Briefly for a particular test case, PIV provides a time sequence of N_t two-dimensional instantaneous velocity fields available at (n_y x n_z) PIV grid points. As a first step, the Reynolds decomposition is applying providing the fluctuating part of the instantaneous velocity field. The second step consists in performing POD from the available instantaneous fluctuating part of the velocity field. Using the vectorial snapshot formulation of POD procedure, a discrete series of N_t POD eigenfunctions is obtained via the resolution of the Fredholm equation (equation 1) associated with the temporal correlation tensor. Finally each instantaneous PIV velocity field is projected onto each POD temporal coefficient and large scale energetic flow structures can be isolated with the first POD modes. Details on similar POD application from PIV database can be found in Druault *et al.* (2005). Then by projecting instantaneous velocity field onto the first POD modes, coherent structure events can then be isolated.

4. Results and discussion

4.1 Characterization of the movement of the bottom trawl

A preliminary analysis consists in examining the movement of the bottom trawl. As it has been noted previously (see Fig. 4 and 5), the trawl is free to move in the three directions. The movement of the trawl comes from the turbulence of the flow and the vortex emission. Note that to our knowledge, there are no papers which address the analysis of the instability of the shear layer separating a body having 3 degrees of freedom. This is possible in our work because of the net deformation of the trawl. To illustrate the movement of the trawl, Fig. 6 presents the time evolution of a fixed y-point located on the surface of the trawl. A transverse (z-direction) movement can be then identified even if the chaotic movement of the trawl is evident. Recall that the movement of the trawl in the third direction can not be taken into account from 2D PIV measurements. Fig. 6 also represents the corresponding FFT (Fast Fourier Transform) computed from the time signal. The transverse movement of the trawl corresponds then to a frequency of f_0=0.055Hz. Then, such frequency can be associated with a Strouhal number ($S_t=f_0\ d_0\ /\ U_{ref}$) of 0.2. This number is computed from the reference velocity U_{ref}=0.54m/s and a mean length of modelled bottom trawl which is approximately: d_0=0.02m. Some comments on this result will be provided in the section 4-4.

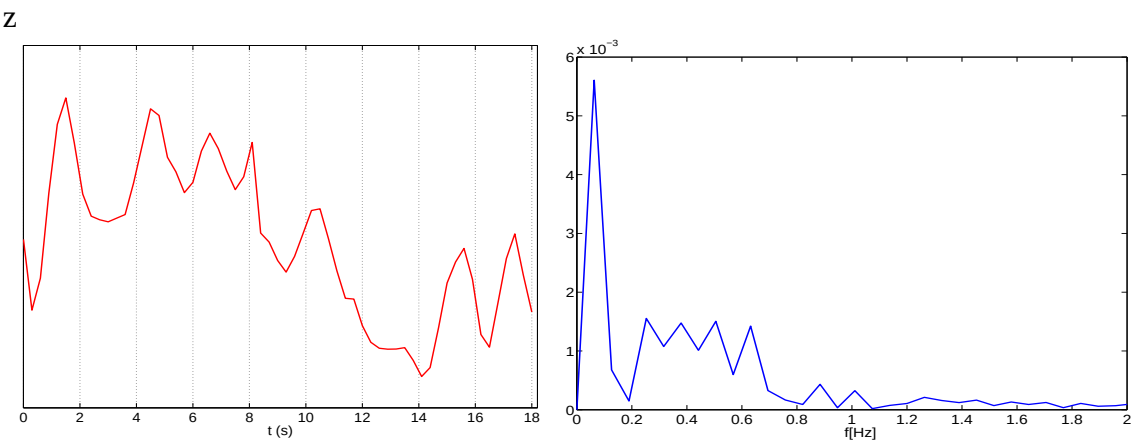

Fig. 6: Moving bottom trawl measurements. Left hand side, Time evolution of a y-point located on the bottom trawl along the z direction. Right hand side, corresponding spectral representation.

4.2 Mean Flow analysis

A preliminary investigation of both flow configurations is performed from mean flow analysis. Based on rigid cod-end experimental flow configuration, Fig. 7 presents the mean flow field and the normalized turbulent kinetic energy obtained from previous analysis (Bouhoubeiny *et al.*, 2010). The turbulent kinetic energy is computed from the available 2D fluctuating velocity fields. On these figures, the vertical patterns of the wake are clearly visible. Indeed, the near wake of the porous structure is dominated by two large counter rotating vortices which are symmetric along the *z=0* axis (Fig. 7). Also, the turbulent wake is clearly identified showing the separated shear layer. Note that the turbulent kinetic energy levels in the upper part of the wake are superior to the ones obtained in the bottom part. This is explained by the experimental device. Indeed, the rigid cod-end trawl is located near the bottom wall of the experimental flume tank. The presence of the wall may corrupt the kinetic energy distribution in this zone. As a consequence, in the following to avoid any misunderstanding, the large scale flow structure investigation will be performed in the upper part of the rigid cod-end.

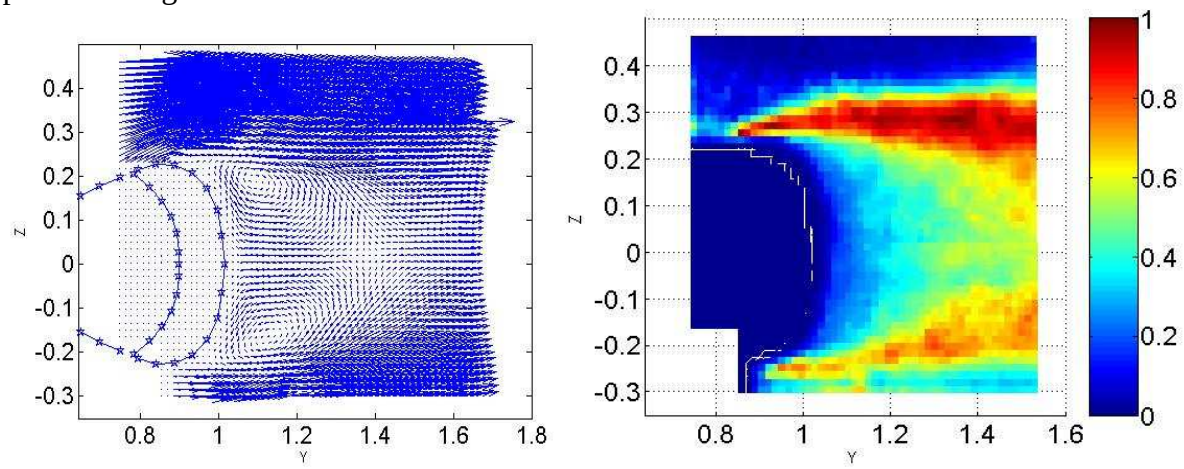

Fig. 7: Rigid cod-end measurements. Left hand side, mean flow field. Right hand side, normalized turbulent kinetic energy.

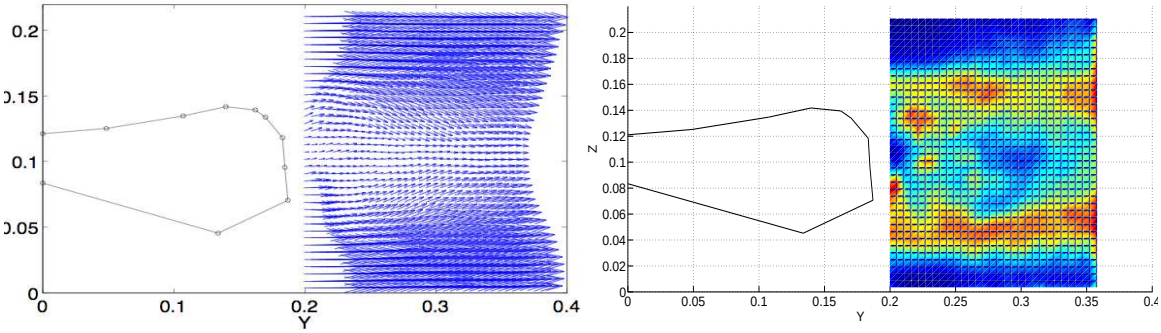

Fig. 8: Moving bottom trawl measurements. Left hand side, mean flow field. Right hand side, normalized turbulent kinetic energy.

Mean flow analysis deduced from the analysis of flow around moving trawl is presented on Fig. 8. It is then clear that the mean flow structure representation is quite different than the one deduced from the rigid cod-end. In a similar way, the turbulent kinetic energy is not located in a precise zone due to the movement of the trawl. It is then possible to identify the upper and lower z-limits of the trawl movement (Fig. 8). By comparing these results to the ones deduced from the rigid cod-end flow configuration, the unsteady turbulent flow due to the movement of the trawl is clearly indicated.

4.3 Proper Orthogonal Decomposition analysis

Based on each database associated with a particular measurement plane, a similar procedure is performed to extract the large scale flow structures of the flow with the aid of POD procedure. In each case, POD is performed from the fluctuating velocity field deduced from the classical Reynolds decomposition.

Note that rigid cod-end measurements and moving bottom trawl measurements allow the determination of 500 and 272 POD modes respectively. These numbers are directly related to the number of PIV snapshots available in each flow configuration (sections 2-3-1 and 2-3-2).
Fig. 9 presents the POD energy convergence deduced from selected results. First, two PODs named POD_1 and POD_2 are computed from the rigid cod-end measurements obtained in planes 1 and 2 respectively. Then, on the left hand side of this Fig., the resulting POD_1 mode energy content is superimposed onto the POD_2 one. Note on this Fig. the x-axis is limited to 150 in order to better appreciate the energetic content of the first POD modes. We then observe that the energy content is quasi similar is both planes traducing that the energetic flow organization is similar in each plane. Thus, the first POD_1 mode and the first 6 ones contains respectively 32% and 63% of the total kinetic energy. On the right hand side of Fig. 9, previous energy content is superimposed to the one deduced from the POD computed from moving bottom trawl measurements. Thus, even if only 272 POD modes are available (compared to the 500 ones available when dealing with rigid cod-end measurements), the POD energy convergence is great slower in this second flow configuration. Indeed, in this last case, the first POD mode and the first 6 modes contain 21% and 38% of the total kinetic energy respectively. Such result is directly related to the unsteady character of the flow due to the trawl movement. The resulted flow organization differs then greatly to the one deduced from the rigid cod-end measurements.

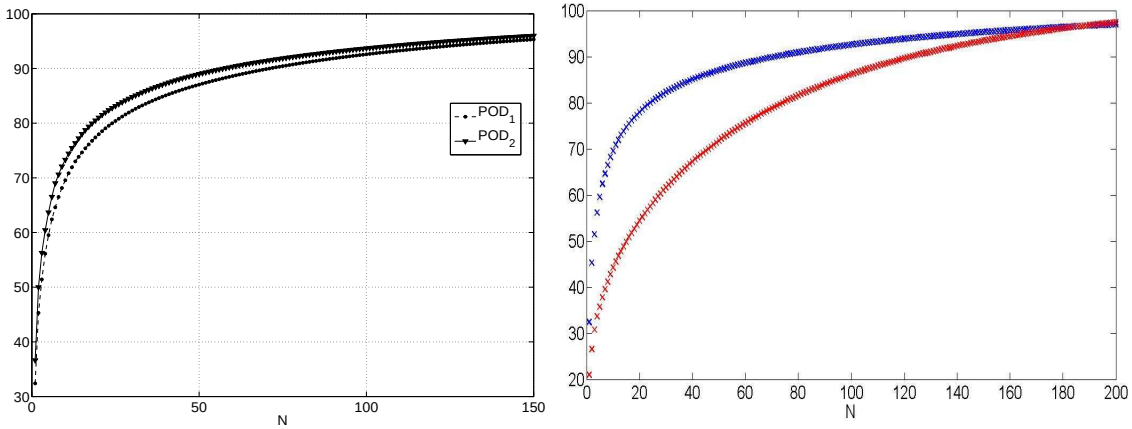

Fig. 9: POD energy convergence. Left hand side: POD computed from rigid cod-end measurements in planes 1 and 2; Right hand side: POD computed from moving bottom trawl measurements (red symbol) superimposed onto POD computed from rigid cod-end measurements (plane 1).

An illustration of the potential of POD application is given on Fig. 10. Based on rigid cod-end measurements, an instantaneous vector field is plotted and also its projection onto the first 6 POD modes. It is observed that large scale energetic flow structures embedded in the background turbulent flow are clearly extracted from the instantaneous velocity snapshot. Then spatial flow structures are extracted from both flow configurations and the extent of these flow structures could be analyzed as a function of the movement or not of the trawl.

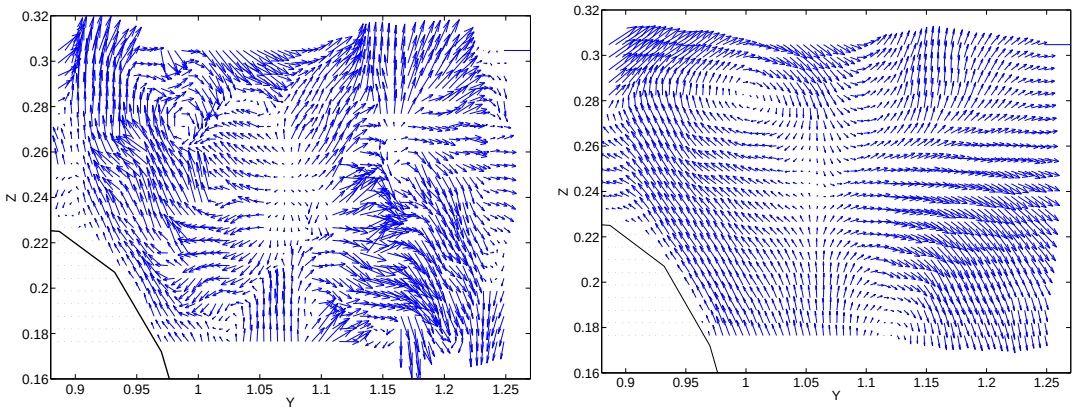

Fig. 10: Rigid cod-end measurements (Plane 1). Left hand side, instantaneous vector velocity field. Right hand side, the same instantanesous velocity field projected onto the first 6 POD modes.

POD can be used to detect not only instantaneous flow structures, but also the frequencies associated with the flow structures. Thus spectral analysis of the large scale flow structures is performed in the following.

4.4 Spectral analysis

A frequency analysis of the vortex shedding frequency is now performed from both flow configurations. Such analysis associated with a porous structure has not yet been fully investigated. Due to the difficulty in properly numerically modeling trawl or related fishing nets, such investigation can then be performed essentially from experimental measurements.

Recall that both flow configurations have an input constant streamwise velocity component of U_{ref} = 0.54 m/s. The reference lengths associated with the cod-end and the bottom trawl are d=0.454m and d_0=0.2m respectively. These reference velocity and lengths are used to compute the associated Strouhal numbers.

Based on previous rigid cod-end measurements (Bouhoubeiny *et al.*, 2010), the spectra of the streamwise velocity stored in the beginning of the wake of the rigid cod-end flow exhibit maxima peaks corresponding to a Strouhal number of 0.27. These values are directly related to the flow instabilities of the boundary layer and the shear layer. Conversely, the power spectra computed in the wake (point P2 in Fig. 11, left hand side) shown a typical frequency corresponding to a Strouhal number of 0.185. This is associated with the Kelvin-Helmhotz instability in the detached shear layers. This Strouhal number is similar to the one obtained in the wake of flow behind a cylinder or and sphere. On the left hand side of Fig. 12, an illustration of the power spectrum computed from raw available measurements stored at P2 position is given.

In this paper, the power spectrum of the streamwise velocity component computed at a selected location behind the moving bottom trawl is investigated. This location (point P1) is given on Fig. 11. Fig. 13 (left hand side) presents the corresponding power spectrum deduced from raw available database. The maxima peak corresponds to a frequency of 0.055 that is a Strouhal number of 0.02. This frequency corresponds to the one associated with the movement of the trawl (see Fig. 6). Also this Strouhal number is similar to the one obtained in the wake behind the rigid cod-end.

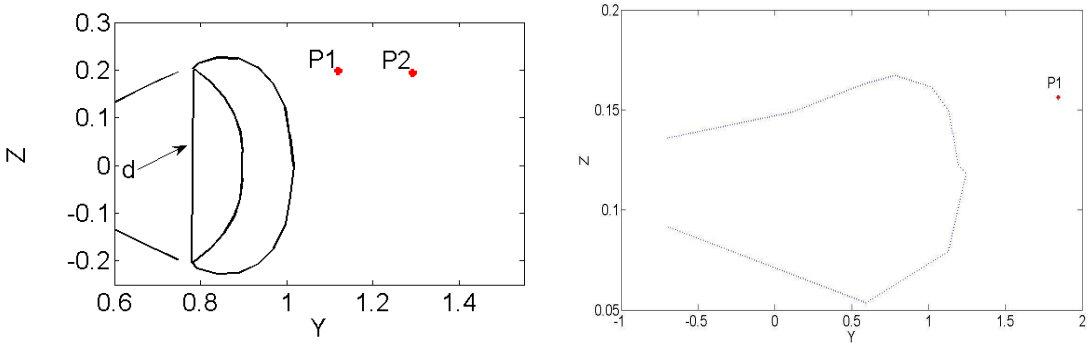

Fig. 11: Space locations from which instantaneous streamwise velocities are stored to compute their corresponding power spectra. Left hand side: rigid cod-end measurements. Right hand side: Moving bottom trawl measurements.

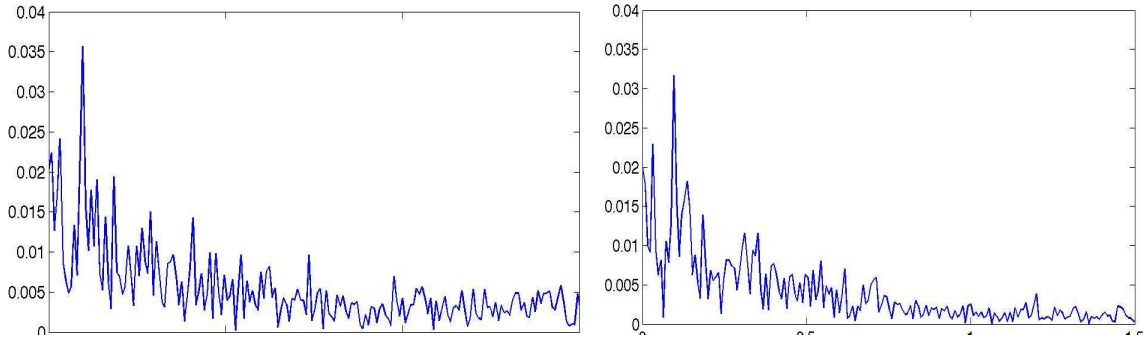

Fig. 12: Rigid cod-end measurements obtained at P2 position (see Fig. 11). Left hand side: Power spectrum of the u velocity component from raw PIV database; Right hand side: Power spectrum the u velocity component projected onto the first 6 POD modes.

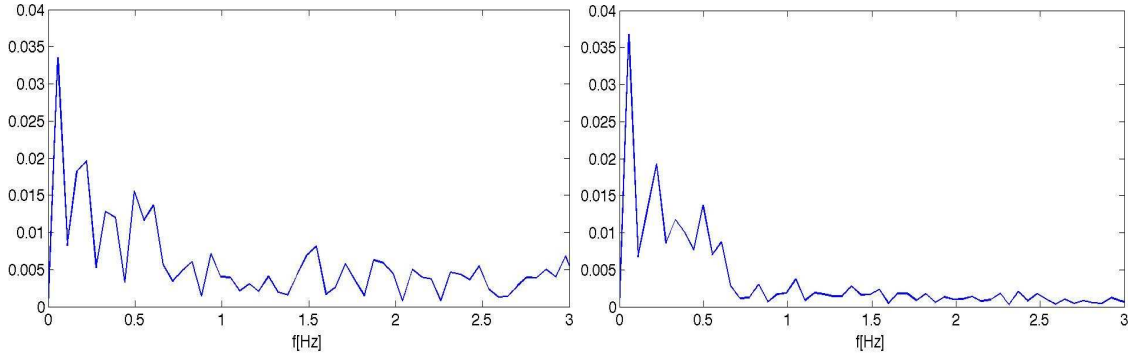

Fig. 13: Moving bottom trawl measurements obtained at P1 position (see Fig. 11) Left hand side: Power spectrum of the u velocity component from raw PIV database; Right hand side: Power spectrum the u velocity component projected onto the first 3 POD modes.

In each flow configuration, instantaneous velocity fields stored at selected location are now projected onto the associated first POD modes. Power spectra are then computed from these velocity fields. Fig. 12 and 13 (right hand side) present the power spectra of the streamwise velocity projected onto 6 and 3 POD modes respectively. Recall that the first 6 POD_1 modes correspond to 63% of the total energy, and the first 3 POD modes correspond to 32% of the total energy in this flow configuration. It is then observed that in each flow configuration, the first POD modes contains the information associated to the vortex shedding phenomenon.

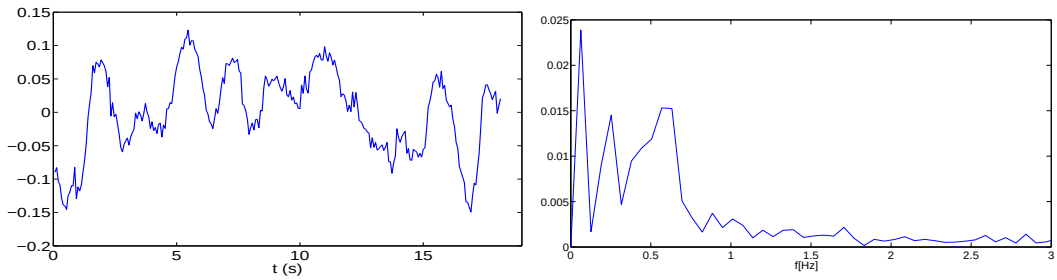

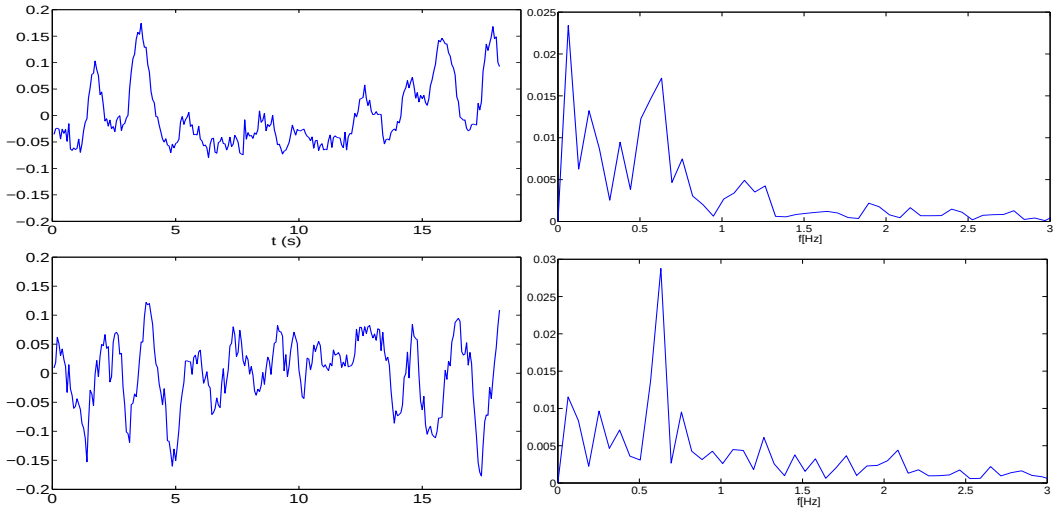

Fig. 14: Moving bottom trawl measurements. Top to Bottom : first, second and third POD modes. Left hand side, Time evolution of POD coefficients. Right hand side, Corresponding FFT signal.

For further investigation the POD application, the analysis of the temporal POD coefficients is performed. Fig. 14 presents the time evolution of the first 3 POD coefficients computed from moving trawl measurements. The FFT transform of each temporal coefficient is computed and also presented on Fig. 14. It is observed that the first 2 modes clearly exhibit the main frequency peak associated with the Strouhal number of 0.2. Conversely, a similar analysis using the rigid cod-end measurements shows that only the first POD mode exhibits the typical vortex shedding frequency. POD is then shown to be effective as a filter for such frequency analysis.

5. Conclusions

Flow field measurements behind a rigid cod-end and a moving bottom trawl are conducted using Time Resolved PIV method. Such a method is based on an image acquisition rate allowing the time resolved sampling of the vortex shedding phenomenon. These experiments form one of the first studies in which i) the main flow characteristics around fishing net structure are investigated and ii) the analysis of the instability of the shear layer separating a body having 3 degrees of freedom is performed.

Furthermore, it is demonstrated the effectiveness of the POD procedure to extract not only the large scale spatial flow structures but also their associated frequencies. POD is shown to be robust to act as a filter for the frequency analysis.

It is also demonstrated that the vortex shedding phenomenon obtained behind a rigid cod-end has some similarities with the one behind a cylinder with a Strouhal number approaching 0.2. Also, even if the moving bottom trawl is subjected to move in the three directions, we shown that the transverse movement of the trawl can be related to the vortex shedding flow instability deduced from a fixed porous structure.

Finally, this new experimental database can be also used to validate numerical results as well as numerical model.

References

Bouhoubeiny E, Germain G, Druault Ph (2010) Experimental analysis of the characteristics of the flow around bottom trawls. Presented at the 1st Int. Symp. on Fishing Vessel Energy efficiency, Vigo, Spain May 2010.

Dahm E, Wienbeck H, West CW, Valdemarsen JW, O'Neill FG, On the influence of towing speed and gear size on the selective properties of bottom trawls. Fisheries Research 55 (2002) 103-119.

Druault Ph, Guibert Ph, Alizon F (2005) Use of Proper Orthogonal Decomposition for time interpolation from PIV data. Exp. Fluids 39:1009-1023.

Germain G, Druault Ph, Lewandowski R, Vincent B, Billard J.Y. (2010) HydroPêche: a way to improve energy efficiency of fishing devices. Presented at the 1st Int. Symp. on Fishing Vessel Energy efficiency, Vigo, Spain May 2010.

Govardhan RN, Williamson CHK (2005) Vortex-induced vibrations of a sphere. J. Fluid Mech. 531: 11-47.

Holmes P, Lumley JL, Berkooz G (1996) Turbulence, coherent structures, dynamical systems and Symmetry. Cambridge monograph on mechanics eds.

ISO 1107-1974 Fishing nets-netting-basic terms and definitions. International Standards Organisation.

Lumley J (1967) The structure of inhomogeneous turbulent flows, in: Atmospheric Turbulence and Radio Wave Propagation, Yaglom and Tatarsky eds. :166-178.

Meyler L, Simulation of net structures hydrodynamic fields. Modelling and Simulation, 2008.

O'Neill FG, O'Donoghue T (1997) The fluid dynamic loading on catch and the geometry of trawl cod-ends. Proc. R. Soc. Lond. A 453, 1631-1648.

O'Neill FG, Knudsen LH, Wileman DA, McKay SJ, Cod-end drag as a function of catch size and towing speed. Fisheries Research 72 (2005) 163-171.

Perrin R. Braza M, Cid E, Cazin S, Barthet A, Sevrain A, Mockett C, Thiele F (2007) Obtaining phase averaged turbulence properties in the near wake ofa circular cylinder at high Reynolds number using POD. Exp. Fluids 43: 341-355.

Pichot G, Germain G, Priour D (2008) On the experimental study of the flow around a fishing net. Eur. J. Mech. B/Fluids 28: 103-116.

Priour D, Numerical optimisation of trawls design to improve their energy efficiency. Fisheries Research 98 (2009) 40-50.

Sirovich L (1987) Turbulence and the dynamics of coherent structures. Part I: Coherent structures. Q. Appl. Math. XLV:561:571.

Van Oudheusden BW, Scarano F, Van Hinsberg NP, Watt DW (2005) Phase-resolved characterization of vortex shedding in the near wake of a square-sectioncylinder ar incidence. Exp. Fluids 39 : 86-98.

Williamson CHK, Govardhan R, (2004) Vortex induced vibrations. Ann. Rev. Fluid Mech. 36: 413-455.